A Machine Learning Regularization of the Inverse Problem in Electrocardiography Imaging

Nejib Zemzemi[1], Remi Dubois[2], Yves Coudière[1], Olivier Bernus[2], Michel Haissaguerre[3]

[1] INRIA, Bordeaux, France
[2] IHU LIRYC, PTIB - Hôpital Xavier Arnozan, Pessac, France
[3] Hôpital cardiologique du Haut Lévèque, Pessac, France

Abstract

Radio-frequency ablation is one of the most efficient treatments of atrial fibrillation. The idea behind it is to stop the propagation of ectopic beats coming from the pulmonary vein and the abnormal conduction pathways. Medical doctors need to use invasive catheters to localize the position of the triggers and they have to decide where to ablate during the intervention. ElectroCardioGraphy Imaging (ECGI) provides the opportunity to reconstruct the electrical potential and activation maps on the heart surface and analyze data prior to the intervention. The mathematical problem behind the reconstruction of heart potential is known to be ill posed. In this study we propose to regularize the inverse problem with a statistically reconstructed heart potential, and we test the method on synthetically data produced using an ECG simulator.

1. Introduction

Different methods based on Tikhonov regularization [1] have been used in order to regularize the inverse problem in electrocardiography imaging, but still the reconstructed electrical potential is not sufficiently satisfactory. Previous work [2] presented a machine learning technique based on a Reproducing Kernel Hilbert Space (RKHS). This method allows a good capturing of the activation times but it has been reported in [2] that the value of the reconstructed electrical potentials is not sufficiently accurate in terms of amplitude. In this work we use the machine learning solution as a regularization term in the least square classic formulation of the inverse problem and we show how it improves the reconstruction. We propose to compare different formulations of the inverse problem: a) Least square with Tikhonov regularization, b) Statistical RKHS, c) Least square regularized with the statistical RKHS solution, d) Least square regularized with the nearest solution in a data base.

In order to assess and compare these methods, we need first to create synthetic data on which will test these different approaches. In paragraph 2.1, we present the forward problem used to simulate potential in the atria surface and in the torso. We simulate a data base following different stimulation position on the atria. This data base will be used in paragraph 2.2 to train the statistical model for the methods b) and c) and to choose the nearest solution in method d).

2. Methods

In this section we present the models used to simulate the forward problem and the methods used to solve the inverse problem. In addition, to solve the inverse problem we need data of electrical potential on the body surface. These data are constructed using 3D mathematical models simulating the electrical activity in the heart and in the torso.

2.1. Forward problem

The bidomain equations were used to simulate the electrical activity of the heart and extracellular potentials in the whole body (see *e.g.* [3–5]). These equations in the heart domain Ω_{H} are given by:

$$\begin{cases} A_{\mathrm{m}}\big(C_{\mathrm{m}}\dot{V}_{\mathrm{m}} + I_{\mathrm{ion}}(V_{\mathrm{m}},\boldsymbol{w})\big) - \operatorname{div}\big(\boldsymbol{\sigma}_{\mathrm{i}}\boldsymbol{\nabla}V_{\mathrm{m}}\big) \\ \qquad\qquad = \operatorname{div}\big(\boldsymbol{\sigma}_{\mathrm{i}}\boldsymbol{\nabla}u_{\mathrm{e}}\big) + I_{\mathrm{stim}}, \\ -\operatorname{div}\big((\boldsymbol{\sigma}_{\mathrm{i}}+\boldsymbol{\sigma}_{\mathrm{e}})\boldsymbol{\nabla}u_{\mathrm{e}}\big) = \operatorname{div}(\boldsymbol{\sigma}_{\mathrm{i}}\boldsymbol{\nabla}V_{\mathrm{m}}), \\ \qquad \dot{\boldsymbol{w}} + \boldsymbol{g}(V_{\mathrm{m}},\boldsymbol{w}) = 0, \\ \qquad \boldsymbol{\sigma}_{\mathrm{i}}\boldsymbol{\nabla}V_{\mathrm{m}}\cdot\boldsymbol{n} = -\boldsymbol{\sigma}_{\mathrm{i}}\boldsymbol{\nabla}u_{\mathrm{e}}\cdot\boldsymbol{n} \quad \text{on } \Sigma. \end{cases} \tag{1}$$

The state variables V_{m} and u_{e} stand for the transmembrane and the extra-cellular potentials. Constants A_{m} and C_{m} represent the rate of membrane surface per unit of volume and the membrane capacitance, respectively. I_{stim} and I_{ion} are the stimulation and the transmembrane ionic currents. The heart-torso interface is denoted by Σ. The intra- and extracellular (anisotropic) conductivity tensors, $\boldsymbol{\sigma}_{\mathrm{i}}$ and $\boldsymbol{\sigma}_{\mathrm{e}}$, are given by $\boldsymbol{\sigma}_{\mathrm{i,e}} = \sigma^{\mathrm{t}}_{\mathrm{i,e}}\boldsymbol{I} + (\sigma^{\mathrm{l}}_{\mathrm{i,e}} - \sigma^{\mathrm{t}}_{\mathrm{i,e}})\boldsymbol{a}\otimes\boldsymbol{a}$, where $\boldsymbol{a}$ is a unit vector parallel to the local fiber direction and $\sigma^{\mathrm{l}}_{\mathrm{i,e}}$ and

$\sigma^{\mathrm{t}}_{\mathrm{i,e}}$ are, respectively, the longitudinal and transverse conductivities of the intra- and extra-cellular media. The field of variables $\boldsymbol{w}$ is a vector containing different chemical concentrations and various gate variables. Its time derivative is given by the vector of functions $\boldsymbol{g}$.

The precise definition of $\boldsymbol{g}$ and I_{ion} depend on the electrophysiologic transmembrane ionic model. In the present work we make use of one of the biophysically detailed human ventricular myocyte model [6]. The ion channels and transporters have been modeled on the basis of the most recent experimental data from human ventricular myocytes.

Figure 1 provides a geometrical representation of the domains considered to compute extracellular potentials in the human body. In the torso domain Ω_{T}, the electrical potential u_{T} is described by the Laplace equation.

$$\mathrm{div}(\boldsymbol{\sigma}_{\mathrm{T}}\boldsymbol{\nabla} u_{\mathrm{T}}) = 0, \quad \text{in} \quad \Omega_{\mathrm{T}}, \tag{2}$$

where $\boldsymbol{\sigma}_{\mathrm{T}}$ stands for the torso conductivity tensor. For the boundary condition, we suppose that The torso is isolated so in the external boundary we have:

$$\boldsymbol{\sigma}_{\mathrm{T}}\boldsymbol{\nabla} u_{\mathrm{T}} \cdot \boldsymbol{n}_{\mathrm{T}} = 0, \quad \text{on} \quad \Gamma_{\mathrm{ext}}, \tag{3}$$

where $\boldsymbol{n}_{\mathrm{T}}$ is the outward unit normal to the torso external boundary Γ_{ext}. On the internal boundary which is the heart torso interface, we suppose that we have continuity of electrical potential

$$u_{\mathrm{e}} = u_{\mathrm{T}}, \quad \text{on} \quad \Sigma. \tag{4}$$

From (2)-(3)-(4) we obtain the well posed model in the torso

$$\begin{cases} \mathrm{div}(\boldsymbol{\sigma}_{\mathrm{T}}\boldsymbol{\nabla} u_{\mathrm{T}}) = 0, & \text{in} \quad \Omega_{\mathrm{T}}, \\ \boldsymbol{\sigma}_{\mathrm{T}}\boldsymbol{\nabla} u_{\mathrm{T}} \cdot \boldsymbol{n}_{\mathrm{T}} = 0, & \text{on} \quad \Gamma_{\mathrm{ext}}, \\ u_{\mathrm{e}} = u_{\mathrm{T}}, & \text{on} \quad \Sigma. \end{cases} \tag{5}$$

We use finite element method in order to solve equations (1) and (5), a space discretisation of the heart and torso domains is then needed. Since we are interested in targeting ectopic beats in the atria, we only consider the electrical activation in the atria. The finite element geometry of atria is given in Figure 2.1 (left). it was embedded in a torso geometry given in Figure 2.1 (right) [7].

2.2. Inverse problem

In this section we present the different methods used to solve the inverse problem. The RKHS method has been purely used to reconstruct statistical solution of the inverse problem see [2] from a set of precomputed EGMs and body surface potentials (BSPs). It has been also reported in [8] that RKHS method could be successfully used to reconstruct BSPs from EGMs provided that a sufficiently rich data set is given. There two important phases in the RKHS

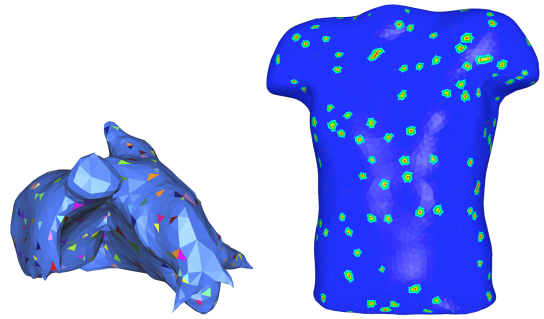

Figure 1. Finite element computational domains: Atria geometry with the different locations of stimulus used to construct the training data set (lfet). Torso geometry with different BSP measurements locations (right).

method, the first is the learning phase and the second is the reconstruction phase. For the sake of simplicity we briefly recall these two phases, we refer to [2] for readers interested in more details. In the learning phase we need a data set consisting of couples of BSPs and EGMs. Let's denote this data set by $(BSP_i, EGM_i)_{i=1\ldots n}$.

The main goal is to build a function f able to accurately map a BSP to an EGM. We use a kernel ridge regression method based on the Gaussian kernel

$$K(\mathbf{x},\mathbf{y}) = \mathbf{e}^{-\frac{|\mathbf{x}-\mathbf{y}|^{\mathbf{2}}}{\mathbf{2}\sigma^{\mathbf{2}}}}, \quad \forall \mathbf{x},\mathbf{y} \in \mathbb{R}^{\,m\times p}.$$

We look for f in a RKHS $(\mathcal{H}, \langle\cdot,\cdot\rangle_{\mathcal{H}})$ characterized by the following property,

$$\forall f \in \mathcal{H}, \quad \forall \mathbf{x} \in \mathbb{R}^{\,m\times p}, \quad f(\mathbf{x}) = \langle \mathbf{f}(\cdot), \mathbf{K}(\cdot,\mathbf{x})\rangle_{\mathcal{H}}. \tag{6}$$

where $\langle\cdot,\cdot\rangle_{\mathcal{H}}$ is the inner product in $\mathcal{H}$. For given bsp the statistical EGM is computed as follows

$$\tilde{egm} = f(bsp) := \sum_{i=1}^{n} \alpha_i K(bsp, BSP_i). \tag{7}$$

Details about how to find $(\alpha_i)_{i=1\ldots n}$ could be found in [2]. The inverse problem in electrocardiography is widely formulated using the least square approach a) minimizing the flowing objective function :

$$J(U(t)) = \| M * U(t) - bsp(t) \|_{l^2} + \lambda \| U(t) \|_{l^2}, \tag{8}$$

where M is the transfer matrix computed using finite element method as in [9] (section 5.5.1) and λ is the Tikhonov regularization parameter. We propose to compare the solution of this formulation to the RKHS solution given by equation (7) method b). We also propose to compare it with following formulation c)

$$\begin{aligned} J(U(t)) = &\| M * U(t) - bsp(t) \|_{l^2} \\ &+ \lambda \| U(t) - f(bsp)(t) \|_{l^2}, \end{aligned} \tag{9}$$

This means that we regularize with the statistical solution computed using the RKHS approach. In the last method d) we propose to compare with is a regularization with the nearest EGM in the data base.

$$J(U(t)) = \| M * U(t) - bsp(t) \|_{l^2} + \lambda \| U(t) - EGM_j(t) \|_{l^2}, \quad (10)$$

where the index j

$$j = \min_{i \in \{1,\ldots,n\}} \| BSP_i - bsp \|_{l^2} .$$

This would allow us to assess whether or not it is worth reconstructing a statistical solution and plug it into the regularization term, or is it enough to take the EGM corresponding to closest BSP in the data base and regularize with, instead of statistically reconstructed.

3. Results

In this section we present simulations of the inverse problems for the methods we presented in the previous paragraph. In order to construct the statistical solution that is used in methods b) and c) and the nearest solution in method d), we built 400 cases of heart beats each one corresponds to a different stimulation position. This data base is used to train the statistical model, we then obtain a metamodel (the function f). We simulated a heart beat which does not belong to the training data set, we extracted the body surface potential from the forward solution and aim to recover the electrical potential on the atria using each of the four methods that we presented. We extract the time course of the potential in two points in the atria and compare the different methods.

In Figure 2, we show a comparison of the time course of the electrical potential in the node number 100 of the atria. The red (and continuous) line stands for the exact solution which was computed from the forward solution. The purple (and dotted) line stands for the method a) least square with zero Tikhonov regularization. The green line (and dashed) is the RKHS solution, the blue line (and dotted) is the least square regularized with RKHS solution and the cyan line (dashed and dotted) stands for the least square regularized with the nearest solution in the data base. First we can see the method c) improves the solution given by the method b) in terms of amplitude. The solution given by method d) is shifted and does not have the same amplitude as the exact solution. The shifting is more pronounced and achieves more than 20ms in Figure 3 (where the time course of the potential is extracted from node 200), this would highly affect the activation time reconstruction.
We also remark that the obtained potential with the standard Tikhonov regularization (method a) smooths the inverse solution too much, and it is very clear in figure 3, this also may significantly affect the activation map since

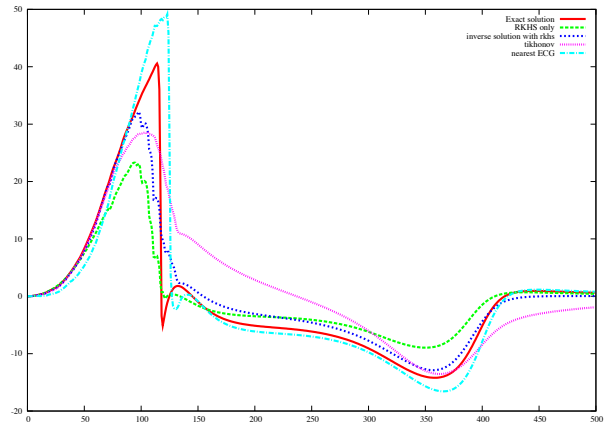

Figure 2. Electrical potential at node 100 (see text).

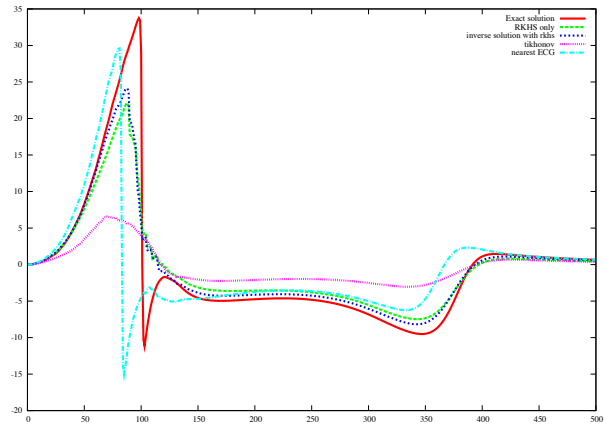

Figure 3. Electrical potential at node 100 (see text).

the maximum time derivative could be highly altered. In Figure 4 we show the activation time maps obtained using the different methods. We compute the activation times following maximum time derivative at each node of the mesh. The exact activation map (top, left image in Figure 4) is obtained from the forward problem solution. Both of activation maps computed from method b (respectively c) solutions are accurate, both of them localized the ectopic stimuli. Activation times obtained by method d) are far from the exact solution, this explains the time shifting in the electrical potential depolarization (Figures 2 and 3). The activation map computed using method a) is highly altered compared to the exact solution its values reach 179 ms while the last depolarized cell in the exact solution is at 142 ms. This means that as some places the error could be more than 37 ms.

4. Discussion

In this work we showed that the machine learning technique is a good approach to regularize the inverse problem in electrocardiography. The inverse solution solution was improved when we plugged it into the regularization term of the least square problem the statistical solution obtained

using the regression approach (RKHS). We noticed that regularizing with the nearest solution in the data base is not a good approach. The least square with zero Tikhonov regularization (method a) smooths the inverse solution too much, since it constrains the solution to be as much as possible close to zero even in the height variation condition like in depolarization phase. We have to notice here that the accuracy of the statistical solution depends on the training data set. Nevertheless, even if the statistical solution is not too much accurate, we think that plugging this solution into the regularization term would be better than zero Tikhonov regularization that constrains the solution to be close to zero.

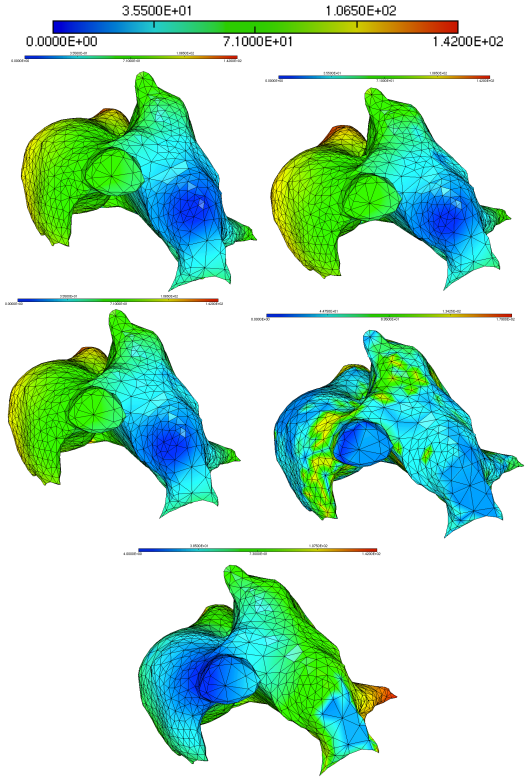

Figure 4. Comparison of the activation times (from left to right and from top to bottom): exact activation times and activation times reconstructed with RKHS metamodel (method b), activation times reconstructed with least square regularized with RKHS solution (method c), activation map reconstructed with Least square with standard Tikhonov regularization (method a) and activation map reconstructed with Least square with nearest ECG regularization.

5. Conclusion

In this work presented a new regularization of the inverse problem in electrocardiography based on a machine learning technique. We use the reproducing kernel Hilbert space regression approach to construct a statistical solution of the inverse problem, we then use this solution to regularize the least square formulation of the inverse problem. Numerical results show that this approach improves the quality of the inverse solution and that among the four methods presented in this paper it gives the best construction of electrical potential in the atria. The different methods have been tested on synthetic data. We used a 3D ECG simulator based on a 3D multiscale mathematical model in order to create this data. Future works will assess the accuracy of this method with clinical data, the ECG simulator could be used in this case in order to enrich the clinical data.

Acknowledgments

This work was partially supported by an ANR grant, part of the *Investissements d'Avenir* program, reference ANR-10-IAHU-04.

References

[1] Ghosh S, Rudy Y. Application of l1-norm regularization to epicardial potential solution of the inverse electrocardiography problem. Annals of Biomedical Engineering 2009; 37(5):902912.

[2] Zemzemi N, Labarthe S, Dubois R, Coudiere Y. From body surface potential to activation maps on the atria: A machine learning technique. In Computing in Cardiology (CinC), 2012. IEEE, 2012; 125–128.

[3] Pullan A, Buist M, Cheng L. Mathematically modelling the electrical activity of the heart. From cell to body surface and back again. World Scientific, 2005.

[4] Sundnes J, Lines G, Cai X, Nielsen B, Mardal KA, Tveito A. Computing the electrical activity in the heart. Springer-Verlag, 2006.

[5] Tung L. A bi-domain model for describing ischemic myocardial D–C potentials. Ph.D. thesis, MIT, 1978.

[6] Ten Tusscher K, Panfilov A. Cell model for efficient simulation of wave propagation in human ventricular tissue under normal and pathological conditions. Physics in medicine and biology 2006;51:6141.

[7] Klepfer R, Johnson C, MacLeod R. The effects of inhomogeneities and anisotropies on electrocardiographic fields:a three-dimensional finite element study. IEEE Eh4BC and CMBEC 1995;.

[8] Ebrard G, Fernández M, Gerbeau JF, Rossi F, Zemzemi N. From intracardiac electrograms to electrocardiograms. models and metamodels. In Ayache N, Delingette H, Sermesant M (eds.), Functional Imaging and Modeling of the Heart, volume 5528 of Lecture Notes in Computer Science. Springer-Verlag, 2009; 524–533.

[9] Zemzemi N. Étude théorique et numérique de l'activité électrique du cœur: Applications aux électrocardiogrammes. Ph.D. thesis, Université Paris XI, 2009. `http://tel.archives-ouvertes.fr/tel-00470375/en/`.